# Effects of Thermal Radiation and Ohmic Heating on Hydromagnetic Maxwell Hybrid Nanofluid Flow

**Francis Kirwa Korir (B.Sc.), Prof. Winfred Mutuku**

**Department of Mathematics and Actuarial Science Degree of Masters of Science (Applied Mathematics) In the School of Pure and Applied Sciences of Kenyatta University**

**DOI: https://dx.doi.org/10.51584/IJRIAS.2025.10100000183**

**Received: 28 October 2025; Accepted: 04 November 2025; Published: 22 December 2025**

## ABSTRACT

The constitutive model for the Maxwell fluid is mostly used in the polymeric industry to model the flow of viscoelastic fluids. Since 2005, fluids properties have been enhanced by the emergence of nanofluids and hybrid nanofluids. Studies on Maxwell hybrid nanofluid have been carried out under different conditions, but the effects of both thermal radiation and ohmic heating on the hydromagnetic Maxwell hybrid nanofluid flow has not been investigated. Motivated by this, this study probes into the role that thermal radiation and ohmic heating plays on a 2-D incompressible hydromagnetic flow of Maxwell hybrid nanofluid; a suspension of both molybdenum disulphide and Silicon dioxide nanoparticles in a Maxwell fluid. The model of the is formulated then transformed into a non-dimensional system using similarity variables. The shooting technique is employed to convert the dimensionless equations to their equivalent initial value problem; which is then solved using MATLAB bvp4c solver. The results show that Grashof number decreases temperature but increases velocity while volume fraction increases temperature but decreases velocity.

## INTRODUCTION

### Background of the study

A fluid is a substance that deforms continuously under the action of a shear force. When the fluid's viscosity remains constant under different amounts of forces it's subjected to, it is labelled as Newtonian. Chloroform, ethyl alcohol, water, benzene, hexane and air constitute such fluids. The other class of fluids are called non-Newtonian. They occur when the fluid's viscosity is varied as it's subjected to different amounts of shearing forces. Casson fluid, Maxwell fluid, Williamson fluid, ketchup, tomato paste, paint, adhesives, quicks and among others make up the non-Newtonian fluids. Notably, non-Newtonian fluids are vastly used in industrial processes. Maxwell fluid, proposed by James Clerk Maxwell in 1867, is a simple viscoelastic model mostly used in the polymeric industry. Polymers are essential in the manufacture of coatings, hydrogels, solar energy, batteries, food preservatives and in drug delivery. Hence, devising a way of making the polymerization process efficient in both energy conservation and cost reduction is of high importance. Another interesting Maxwell fluid is the molten polymers. The interest stems from the fact that in their normal form, they can behave as Newtonian fluid. However, in the molten state, they behave a Maxwell fluids.

Generally, conventional fluids are poor conductors of both electricity and heat. In an attempt to refine the fluid features, nanotechnology, which is the science of adding 1-100nm diameter-solid particles of varied shapes to a fluid, was founded by Choi and Eastman (1995). In the past almost three decades, ground-breaking research has been performed as discussed in the literature review section. Unanimously, researchers agree that hybrid nanofluids show more refined fluid features compared to nanofluids and conventional fluids. Its thermal and electric conductivities coupled with mass transfer performance is superior in every way. Hybrid nanofluid are therefore applied in transformers for efficient electricity transmission, in electronics for effective heat transfer, in the biomedical industry for mass transfer, polymeric industries for both either mass or heat transport, among other industries. Due to the qualities and vast applications of hybrid nanofluids, this proposed research is inclined to work on Maxwell hybrid nanofluid. Therefore, for a hybrid nanofluid to be formed, a pair of suitable nanoparticles must be selected for the hybridization process. Alumina/Copper nanoparticle combination is chosen for this study due to multiple studies pointing out that it's a magnificent combination for efficient heat performance enhancement. Zainal *et al.* (2022) hails this combination for its stability. Further, Jaafar *et al.* (2022) points out that Alumina/Copper is not only stable, but also a good conductor and is corrosion resistant.

In order to explain the phenomena of an electrically conducting fluid behaviour as it goes through a magnetic field, Alfvén (1942) came up with the term hydromagnetics. This hydromagnetics are widely used in various industries like in the generation of electricity and flowmeters design. Considering the electrical conductivity of Maxwell hybrid nanofluid and the presence of a constant perpendicular magnetic field, the fluid flow under examination falls into the category of hydromagnetic flows. Additionally, assuming industrial surfaces are in linear motion, this study aims to investigate the impact of thermal radiation and ohmic heating on a two-dimensional, incompressible, hydromagnetic flow of Maxwell hybrid nanofluid. The nanoparticles used are $Al_2O_3$ and $Cu$.

Thermal radiation refers to the transfer of heat energy through electromagnetic waves, primarily in the infrared spectrum, without the need for a medium. It is governed by the Stefan-Boltzmann law, which states that the radiant heat power emitted by a body is proportional to the fourth power of its absolute temperature (Samuel, 2022). In fluid mechanics, thermal radiation plays a crucial role in heat transfer processes, especially in high-temperature environments where other modes of heat transfer, such as conduction and convection, become less effective (Kigio et al., 2021). Applications of thermal radiation are widespread in various industries, including aerospace, nuclear reactors, and manufacturing. For example, in aerospace engineering, the study of thermal radiation is essential for designing heat shields for spacecraft re-entering Earth's atmosphere (Samuel, 2022). In the field of fluid mechanics, understanding thermal radiation is critical for modelling the heat transfer in fluids exposed to high temperatures, such as in combustion chambers or heat exchangers (Fatunmbi et al., 2020). The accurate modelling of radiation effects allows for better efficiency in energy systems and enhances the safety and performance of engineering applications (Ali et al., 2022).

**Statement of the Problem**

Investigation into the role of thermal radiation on the flow of hybrid Maxwell nanofluid over rotating surfaces, as well as shrinking and stretching surfaces, has garnered significant attention in recent research. However, there has been limited focus on understanding the impact of ohmic heating over a surface that linearly stretches in a magnetic hybrid Maxwell nanofluid context. To address this gap, the proposed work aims to explore the influence of thermal radiation and ohmic heating on hydromagnetic Maxwell hybrid nanofluid flow. The base fluid is the molten polyethylene, with alumina and copper nanoparticles chosen as nanoparticles. This study seeks to provide a clearer understanding of the interactions between heat transfer, fluid flow, and magnetic fields in such systems, offering insights valuable for various industrial applications and theoretical advancements in fluid dynamics.

**Justification of the Study**

Maxwell fluid is a very useful viscoelastic model in the polymeric industry. On its own, its conductivity is poor but when nanoparticles are added, the conductivity and other fluid properties are enhanced significantly. The use of alumina-copper nanoparticle combination has proven to be very effective in the hybridization process due to its stability, magnificent conductivities and resistance to corrosion. As a result, this study uses Maxwell as a base fluid and alumina-copper combination as the nanoparticles. Quite a number of researchers have studied Maxwell hybrid nanofluid but, so far, no researcher has delved into the effects of both thermal radiation and ohmic heating on the hydromagnetic Maxwell hybrid nanofluid yet. Therefore, this proposed study will probe into the effect of thermal radiation and ohmic heating on a hydromagnetic alumina/copper-Maxwell hybrid nanofluid over a surface stretching at a linear pace.

**Objectives**

**General Objective**

This study is aimed at mathematically analysing the effects of thermal radiation and ohmic heating on the hydromagnetic $Al_2O_3/Cu$-Maxwell hybrid nanofluid flow over a linearly stretching surface.

**Specific Objectives**

The specific objectives of this study are to;

i. Formulate the mathematical equations for the fluid flow in the presence of thermal radiation and ohmic heating on hydromagnetic hybrid Maxwell nanofluid flow.

ii. Transform the equations to its non-dimensional form using appropriate similarity variables from existing literature.

iii. Investigate the effects of volume fraction, Eckert number, magnetic field, radiation and other pertinent parameters on the flow velocity and temperature.

**Significance of the Study**

The need for increased energy transmission at a minimal cost is a necessity in industries. Maxwell model is widely used in industries and making its heat transmission efficient is pivotal in polymerization. The aim of this study is to theoretically investigate the impacts that thermal radiation and ohmic heating have on the conductivity of the Maxwell hybrid nanofluid. The results of the study will provide useful information to polymeric industries on how various parameters such as radiation and magnetic parameters should be adjusted during the polymerization processes for maximum efficiency in energy transmission. The importance of this study is multifaceted and far-reaching. By advancing our understanding of energy transmission efficiency in industrial processes, it promises to deliver tangible benefits for industries, the environment, scientific knowledge, and education. As such, it represents a significant contribution to both academic research and practical applications, with the potential to reshape industrial practices and foster a more sustainable future.

## LITERATURE REVIEW

**Introduction**

In this section, already existing literature are discussed in the first section and the gap found is highlighted in the second section.

**Existing Literature**

Nanotechnology is a fast growing, heat and mass transfer enhancement field that was spearheaded by Maxwell (1873). In an attempt to improve a variety of fluid features, Maxwell (1873) added solid particles in a base fluid which were millimetre in size. This upgraded the base-fluid features but had a couple of flaws that were later eliminated when Choi and Eastman (1995) proposed the use of nanoparticles instead. The proposed nanoparticles greatly refined the base-fluid properties, but, with the increasing demand for highly efficient gadgets especially electronics, the demand for a better heat transfer enhancer grew.

Suresh *et al.* (2011) proposed hybrid nanofluids, which, through the past decade's research, have proven to be superior in every way to the nanofluids. Hady *et al.* (2012) studied the impacts of radiation on a hybrid nanofluid over a sheet that is stretching at a non-linear pace. From the study, a surge in the radiation and the non-linear parameters heightened the heat rate performance. Using boundary layer analysis launched by Sakiadis (1961) and Homotopy Based Approach, Farooq *et al.* (2019) uncovered that, for a hydromagnetic Maxwell fluid carrying nanomaterials, increasing the Hartman and Deborah numbers boosts the flow velocity but depreciates the heat transfer performance. Rajesh *et al.* (2020) worked on convective MHD flow over a stretching sheet where the results showcased the superiority of hybrid nanofluids over the nanofluid.

Mutuku (2016) concurs with already existing literature on the enhancement of fluid heat transfer in the presence of nanoparticles. In their study, the use of CuO nanoparticle is found to have the most cooling effect compared to alumina and titanium oxide in Ethylene glycol. In their study, Ali *et al.* (2021) confirms that the addition of two-oxide nanoparticles boosts the flow temperature better than when non-oxide nanoparticles are used. Zainal *et al.* (2022) hails this combination for its stability. Further, Jaafar *et al.* (2022) points out that Alumina / Copper is not only stable, but also a good conductor and is corrosion resistant. Jaafar *et al.* (2022) agrees with Ali *et al.* (2021) and also points out that the use of $Al_2O_3$ / $Cu$ nanoparticle combination is most common since their conductivity is high and the corrosion drawback is eliminated. A duality of solutions is recorded by Jaafar *et al.* (2022) where one is steady and the other result is unsteady. In the analysis of the role of thermal radiation on a rotating magnetic hybrid nanofluid, Asghar *et al.* (2022) reports similar solutions to Jaafar *et al.* (2022) but rebrands the outcomes as either stable or unstable. Further, a growth in the temperature distribution is recorded when the Eckert number and the radiation parameter surge. The study conducted by Zainal *et al.* (2022) on role of radiation on Maxwell hybrid nanofluid in a region of stagnation records similar results as obtained by Asghar *et al.* (2022).

Khan *et al*. (2023) explores the impact of adding nanoparticles to grease by modelling the fluid behaviour using the Maxwell model. The use Maxwell base fluid here showcases the expansive applications of this model in industries since majority of the fluids commonly used display viscoelasticity. Great enhancement in heat transmission is observed with the addition of the nanoparticles in this study. Aside from the major advancement in the heating and cooling of machinery, this research boasts of friction reduction and approximately 3% mass transfer reduction as a result of the presence of nanoparticles. Wang *et al*. (2023) uses the Buongiorno model to further investigate the movement of nanoparticles in the Maxwell fluid under the influence of temperature gradient and Brownian motion. In the study, the interaction of thermal radiation, electromagnetic waves and chemical reactions are explored. The impacts of radiation and the occurring reactions on the flow velocity and temperature are highlighted. This study's results are found to be consistent with those observed by Khan *et al*. (2023) . Vijay & Sharma (2023) further considered the stagnation effects , heat and mass transmission on the Maxwell nanofluid. The model is solved using finite element method and the resulting solution informs us of similar findings to what Wang *et al*. (2023) and Khan *et al*. (2023) already got.

### Established gap

From the review above, it is to our understanding that the investigations into the role of thermal radiation on the flow of hybrid Maxwell nanofluid over rotating surfaces, as well as shrinking and stretching surfaces, has garnered significant attention in recent research. However, there has been limited focus on understanding the impact of thermal radiation coupled with ohmic heating over a surface that linearly stretches in a magnetic hybrid Maxwell nanofluid context. The understanding of thermal radiation and ohmic heating have been found to be crucial in determining the heat insulators to be used in our gadgets and industrial machinery. Motivated to address this gap, the proposed work aims to explore the influence of thermal radiation and ohmic heating on hydromagnetic Maxwell hybrid nanofluid flow. The base fluid is Maxwell, with alumina and copper nanoparticles chosen as nanoparticles. This study seeks to provide a clearer understanding of the interactions between heat transfer, fluid flow, and magnetic fields in such systems, offering insights valuable for various industrial applications and theoretical advancements in fluid dynamics.

## METHODOLOGY

### Introduction

In this section, the assumptions made are presented, the flow geometry is displayed and the flow model is formulated. The model equations are then transformed into a non-dimensional system using similarity variables obtained from existing literature. The numerical techniques used to solve the resulting system of equations is then discussed.

**Formulation of Governing Equations**

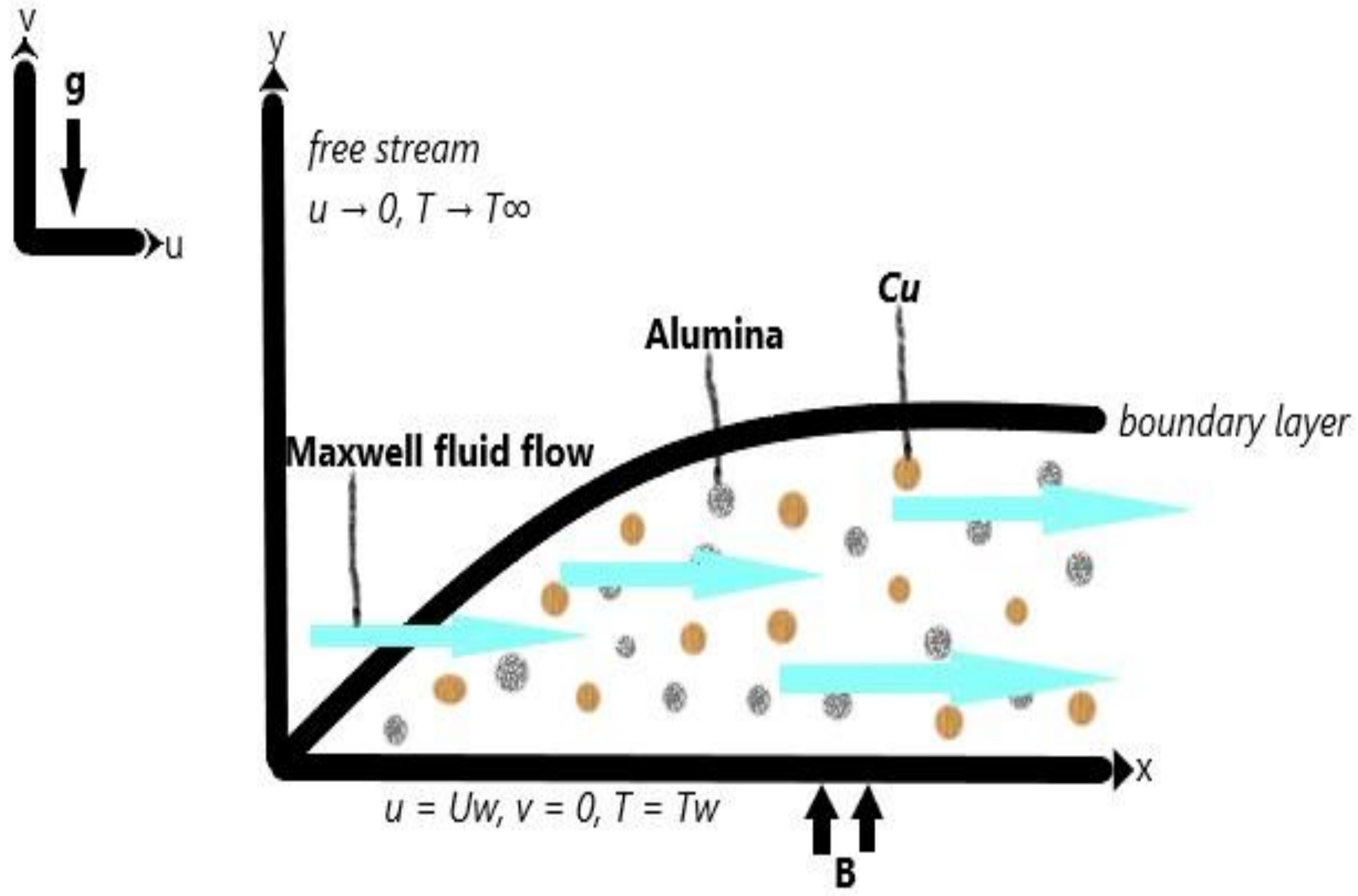


Figure 0.1: Flow geometry

Figure (3.1) displays the 2-D, incompressible flow geometry. Here, a colloidal suspension of $Al_2O_4/Cu$ nanoparticles in Maxwell base fluid form the hybrid nanofluid. The surface is stretching at a linear pace in the direction $x \geq 0$. The flow is experiencing ohmic heating, thermal radiation and a constant perpendicular magnetic field.

The following assumptions are made for the flow under consideration;

1. The flow is an incompressible and steady, and can be represented as a two-dimensional boundary layer flow.
2. The flow occurs over a linearly stretching flat surface along the x-direction, where $x > 0$.
3. A constant perpendicular magnetic field strength is applied to the flow.
4. The no-slip condition is obeyed on the surface.

By modifying Zainal *et al.* (2022) model to incorporate body forces and ohmic heating in the momentum and energy equations respectively, we have the continuity equation as;

$$\frac{\partial u}{\partial x} + \frac{\partial v}{\partial y} = 0 \qquad (3.1.1)$$

ISSN No. 2454-6194 | DOI: 10.51584/IJRIAS |Volume X Issue X October 2025

The hydromagnetic maxwell hybrid nanofluid momentum equation is given as

$$u\frac{\partial u}{\partial x}+v\frac{\partial u}{\partial y}=\mu_{hnf}\rho_{hnf}\frac{\partial^2 u}{\partial y^2}+2\vartheta_f\Lambda\frac{\partial u}{\partial y}\frac{\partial^2 u}{\partial y^2}+g\beta(T-T_\infty)-\frac{\sigma_{hnf}}{\rho_{hnf}}B^2u \qquad (3.1.2)$$

Taking into account the thermal radiation effects, the energy equation is modified to;

$$u\frac{\partial T}{\partial x}+v\frac{\partial T}{\partial y}=\frac{1}{\left(\rho\, C_p\right)_{hnf}}\left(\kappa_{hnf}\frac{\partial^2 T}{\partial y^2}-\frac{\partial q}{\partial y}-Q_0(T-T_w)\right) \qquad (3.1.3)$$

where, the radiative heat flux $q$ is obtained from the Rosseland approximation as;

$$q=-\frac{4\sigma^*}{3k^*}\frac{\partial T^4}{\partial y}$$

From Taylor's series;

$$T^4\approx 4T_\infty^3T-3T_\infty^4$$

Therefore;

$$\frac{\partial q}{\partial y}=-\frac{16\sigma^*T_\infty^3}{3k^*}\frac{\partial^2 T}{\partial y^2}.$$

The boundary equations to capture linear stretching and the no slip conditions are given as

$$u\,(0,x)=ax,\;\; v(0,x)=0,\;\; T(0,x)=T_w. \qquad (3.1.4)$$

where $a\geq 0$, such that, at $a=0$, the surface is immobile and at $a>0$, the surface is stretching. The free stream boundary conditions are;

$$u\,(\infty,x)\to 0,\;\; T(\infty,x)=T_\infty. \qquad (3.1.5)$$

**Effective properties**

The three nanoparticles, each has their thermal and electrical properties, that they contribute to the ternary hybrid nanofluid. The properties of the resulting ternary hybrid nanofluid is referred to as the effective properties. These properties have been estimated in various experimental research and models for the effective properties have been fitted using experimental data. Based on the work of Allehiany *et al.* (2023), the model for the effective thermal conductivity, effective electrical conductivity, effective thermal capacity, effective density and effective viscosity of the ternary hybrid nanofluid are;

$$\frac{\kappa_{hnf}}{\kappa_f}=\frac{2(1-\phi)\phi\,\kappa_f+(1\,+\,2\phi)\,\sum_{i=1}^{2}\phi_i\kappa_i}{(2\,+\phi)\phi\kappa_f\,+\,(1-\phi)\sum_{i=1}^{2}\phi_i\kappa_i}, \qquad (3.2.1)$$

$$\frac{\sigma_{hnf}}{\sigma_f} = \frac{2(1-\phi)\phi\,\sigma_f + (1+2\phi)\sum_{i=1}^{2}\phi_i\sigma_i}{(2+\phi)\phi\sigma_f + (1-\phi)\sum_{i=1}^{2}\phi_i\sigma_i}, \tag{3.2.2}$$

$$(\rho c_p)_{hnf} = (1-\phi)(\rho c_p)_f + \sum_{i=1}^{2}\phi_i(\rho c_p)_i, \tag{3.2.3}$$

$$\rho_{hnf} = (1-\phi)\rho_f + \sum_{i=1}^{2}\phi_i\rho_i, \tag{3.2.4}$$

$$\mu_{hnf} = \mu_f(1-\phi)^{-2}. \tag{3.2.5}$$

and for the sake of simplicity, we rewrite the models as

$$\frac{\kappa_{hnf}}{\kappa_f} = \frac{2(1-\phi)\phi\kappa_f + (1+2\phi)\Sigma_{i=1}^{2}\phi_i\kappa_i}{(2+\phi)\phi\kappa_f + (1-\phi)\Sigma_{i=1}^{2}\phi_i\kappa_i} = A_1 \Rightarrow \kappa_{hnf} = A_1\kappa_f \tag{3.2.6}$$

$$\frac{\sigma_{hnf}}{\sigma_f} = \frac{2(1-\phi)\phi\sigma_f + (1+2\phi)\Sigma_{i=1}^{2}\phi_i\sigma_i}{(2+\phi)\phi\sigma_f + (1-\phi)\Sigma_{i=1}^{2}\phi_i\sigma_i} = A_2 \Rightarrow \sigma_{hnf} = A_2\sigma_f \tag{3.2.7}$$

$$\begin{aligned}(\rho c_p)_{hnf} &= (1-\phi)(\rho c_p)_f + \sum_{i=1}^{2}\phi_i(\rho c_p)_i \\ &= \left(1-\phi+\frac{1}{(\rho c_p)_f}\sum_{i=1}^{2}\phi_i(\rho c_p)_i\right)(\rho c_p)_f \\ &= A_3(\rho c_p)_f\end{aligned} \tag{3.2.8}$$

$$\rho_{hnf} = (1-\phi)\rho_f + \sum_{i=1}^{2}\phi_i\rho_i = \left(1-\phi+\frac{1}{\rho_f}\sum_{i=1}^{2}\phi_i\rho_i\right)\rho_f = A_4\rho_f \tag{3.2.9}$$

$$\mu_{hnf} = 0.904e^{0.148\phi}\mu_f = A_5\mu_f \tag{3.2.10}$$

**Similarity Transformation**

The flow model (3.1.1 -3.1.5) will be transformed to a non-dimensional system of ordinary differential equations using similarity variables

$$\eta = ya^{\frac{1}{2}}\vartheta_f^{-\frac{1}{2}},\quad u = ax\frac{d}{d\eta}f(\eta),\quad v = -a^{\frac{1}{2}}\vartheta_f^{\frac{1}{2}}f(\eta),\quad T = T_\infty + (T_w - T_\infty)\Theta(\eta). \tag{3.3.1}$$

The shooting technique will be employed in the conversion of the resulting dimensionless boundary conditions to their equivalent initial conditions. The shooting technique is used because the method of solution of the resulting ODEs will be numerical techniques. Solving BVPs using numerical techniques is difficult and borderline impossible sometimes, therefore, the shooting technique assists in overcoming this setback. The resulting IVP's approximate solutions will be obtained using RK in MATLAB bvp4c solver. The results will be presented as graphs. The outcomes will be analysed and discussed. Conclusions will be drawn from the study results and suitable recommendations will be presented.

Since $\eta$ is a function of $y$ only, then $\eta_y = a^{\frac{1}{2}}\vartheta_f^{-\frac{1}{2}}$ and $\eta_x = 0$. The first partial derivatives of $u$ with respect to $x$ and $y$ are found as follows;

$$\frac{\partial u}{\partial x} = \frac{d}{dx}\left(ax\frac{d}{d\eta}f(\eta)\right) = a\frac{d}{d\eta}f(\eta)\frac{d}{dx}(x) = a\frac{d}{d\eta}f(\eta)$$

$$\begin{aligned}\frac{\partial u}{\partial y} &= \frac{d}{d\eta}\left(ax\frac{d}{d\eta}f(\eta)\right)\frac{d\eta}{dy} \\ &= ax\frac{d}{d\eta}\left(\frac{d}{d\eta}f(\eta)\right)\frac{d\eta}{dy} \\ &= ax\frac{d^2}{d\eta^2}f(\eta)\frac{d\eta}{dy} \qquad (3.3.3)\end{aligned}$$

The second partial derivative of $u$ with respect to $y$ is as follows;

$$\begin{aligned}\frac{\partial^2 u}{\partial y^2} &= \frac{\partial}{\partial y}\left(\frac{\partial u}{\partial y}\right) = \frac{\partial}{\partial y}\left(ax\frac{d^2}{d\eta^2}f(\eta)\frac{d\eta}{dy}\right) \\ &= \frac{d}{d\eta}\left(ax\frac{d^2}{d\eta^2}f(\eta)\frac{d\eta}{dy}\right)\frac{d\eta}{dy} \\ &= ax\frac{d^3}{d\eta^3}f(\eta)\left(\frac{d\eta}{dy}\right)^2 \qquad (3.3..4)\end{aligned}$$

Next is to consider the first partial derivatives of the variable $v$ with respect $x$ and $y$ are as follows;

$$\begin{aligned}\frac{\partial v}{\partial x} &= 0 \\ \frac{\partial v}{\partial y} &= \frac{\partial}{\partial y}\left(-a^{\frac{1}{2}}\vartheta_f^{\frac{1}{2}}\frac{d}{d\eta}f(\eta)\right) = \frac{\partial}{\partial y}\left(-a^{\frac{1}{2}}\vartheta_f^{\frac{1}{2}}\frac{d}{d\eta}f(\eta)\right)\frac{d\eta}{dy} \\ &= -a^{\frac{1}{2}}\vartheta_f^{\frac{1}{2}}\frac{d}{d\eta}f(\eta)\frac{d\eta}{dy}. \qquad (3.3.5)\end{aligned}$$

The second partial derivative of $v$ with respect to $y$ is as follows;

$$\begin{aligned}\frac{\partial^2 v}{\partial y^2} &= \frac{\partial}{\partial y}\left(\frac{\partial v}{\partial y}\right) = \frac{\partial}{\partial y}\left(-a^{\frac{1}{2}}\vartheta_f^{\frac{1}{2}}\frac{d}{d\eta}f(\eta)\frac{d\eta}{dy}\right) \\ &= \frac{d}{d\eta}\left(-a^{\frac{1}{2}}\vartheta_f^{\frac{1}{2}}\frac{d}{d\eta}f(\eta)\frac{d\eta}{dy}\right)\frac{d\eta}{dy} \\ &= -a^{\frac{1}{2}}\vartheta_f^{\frac{1}{2}}\frac{d}{d\eta}\left(\frac{d}{d\eta}f(\eta)\frac{d\eta}{dy}\right)\frac{d\eta}{dy} \\ &= -a^{\frac{1}{2}}\vartheta_f^{\frac{1}{2}}\frac{d^2}{d\eta^2}f(\eta)\left(\frac{d\eta}{dy}\right)^2 \qquad (3.3.6)\end{aligned}$$

The temperature $T$ is a function of $\Theta$ which is a function of $\eta$ and as a result, $T$ is independent of $x$. The partial derivative of $T$ with respect to $x$ is zero so that

$$\frac{\partial T}{\partial x} = 0,$$

and the partial derivatives of $T$ with respect to $y$ is obtained as

$$\begin{aligned}
\frac{\partial T}{\partial y} &= \frac{\partial}{\partial y}\big(T_\infty + (T_w - T_\infty)\Theta(\eta)\big) = (T_w - T_\infty)\frac{d}{d\eta}\big(\Theta(\eta)\big)\frac{d\eta}{dy} \\
\frac{\partial^2 T}{\partial y^2} &= \frac{\partial}{\partial y}\left(\frac{\partial T}{\partial y}\right) = \frac{\partial}{\partial y}\left((T_w - T_\infty)\frac{d}{d\eta}\big(\Theta(\eta)\big)\frac{d\eta}{dy}\right) \\
&= (T_w - T_\infty)\frac{\partial}{\partial y}\left(\frac{d}{d\eta}\big(\Theta(\eta)\big)\frac{d\eta}{dy}\right) \\
&= (T_w - T_\infty)\frac{d}{d\eta}\left(\frac{d}{d\eta}\big(\Theta(\eta)\big)\frac{d\eta}{dy}\right)\frac{d\eta}{dy} \\
&= (T_w - T_\infty)\frac{d^2}{d\eta^2}\big(\Theta(\eta)\big)\left(\frac{d\eta}{dy}\right)^2 \qquad (3.3.7)
\end{aligned}$$

By substituting $\eta_y$ we have

$$\begin{aligned}
\frac{\partial u}{\partial x} &= a\frac{d}{d\eta}f(\eta) \\
\frac{\partial u}{\partial y} &= ax\frac{d^2}{d\eta^2}f(\eta)\frac{d\eta}{dy} \\
&= ax\frac{d^2}{d\eta^2}f(\eta)\left(a^{\frac{1}{2}}\vartheta_f^{-\frac{1}{2}}\right) \\
&= ax\left(a^{\frac{1}{2}}\vartheta_f^{-\frac{1}{2}}\right)\frac{d^2}{d\eta^2}f(\eta) \\
&= x\sqrt{\frac{a^3}{\vartheta_f}}\frac{d^2}{d\eta^2}f(\eta) \qquad (3.3.8) \\
\frac{\partial^2 u}{\partial y^2} &= ax\frac{d^3}{d\eta^3}f(\eta)\left(\frac{d\eta}{dy}\right)^2 \\
&= ax\frac{d^3}{d\eta^3}f(\eta)\left(a^{\frac{1}{2}}\vartheta_f^{-\frac{1}{2}}\right)^2 \\
&= \frac{a^2 x}{\vartheta}\frac{d^3}{d\eta^3}f(\eta) \qquad (3.3.9)
\end{aligned}$$

$$\begin{aligned}
\frac{\partial v}{\partial x} &= 0 \\
\frac{\partial v}{\partial y} &= -a^{\frac{1}{2}}\vartheta_f^{\frac{1}{2}}\frac{d}{d\eta}f(\eta)\frac{d\eta}{dy} \\
&= -a^{\frac{1}{2}}\vartheta_f^{\frac{1}{2}}\frac{d}{d\eta}f(\eta)\left(a^{\frac{1}{2}}\vartheta_f^{-\frac{1}{2}}\right) \\
&= -a\frac{d}{d\eta}f(\eta). \qquad (3.3.10)
\end{aligned}$$

ISSN No. 2454-6194 | DOI: 10.51584/IJRIAS |Volume X Issue X October 2025

$$\begin{aligned}\frac{\partial^2 v}{\partial y^2} &= -a^{\frac{1}{2}}\vartheta_f^{\frac{1}{2}}\frac{d^2}{d\eta^2}f(\eta)\left(\frac{d\eta}{dy}\right)^2\\ &= -a^{\frac{1}{2}}\vartheta_f^{\frac{1}{2}}\frac{d^2}{d\eta^2}f(\eta)\left(a^{\frac{1}{2}}\vartheta_f^{-\frac{1}{2}}\right)^2\\ &= -\sqrt{\frac{a^3}{\vartheta_f}}\frac{d^2}{d\eta^2}f(\eta). \qquad (3.3.11)\end{aligned}$$

$$\begin{aligned}\frac{\partial T}{\partial y} &= (T_w - T_\infty)\frac{d}{d\eta}\Theta(\eta)\frac{d\eta}{dy}\\ &= (T_w - T_\infty)\left(a^{\frac{1}{2}}\vartheta_f^{-\frac{1}{2}}\right)\frac{d}{d\eta}\Theta(\eta). \qquad (3.3.12)\end{aligned}$$

$$\begin{aligned}\frac{\partial^2 T}{\partial y^2} &= (T_w - T_\infty)\frac{d^2}{d\eta^2}\big(\Theta(\eta)\big)\left(\frac{d\eta}{dy}\right)^2\\ &= \frac{a(T_w - T_\infty)}{\vartheta}\frac{d^2}{d\eta^2}\big(\Theta(\eta)\big) \qquad (3.3.13)\end{aligned}$$

Consider the left hand side of equation (3.1.2) and we have

$$\begin{aligned}LHS &= u\frac{\partial u}{\partial x} + v\frac{\partial u}{\partial y}\\ &= \left(ax\frac{d}{d\eta}f(\eta)\right)\left(a\frac{d}{d\eta}f(\eta)\right) + \left(-a^{\frac{1}{2}}\vartheta_f^{\frac{1}{2}}f(\eta)\right)\left(x\sqrt{\frac{a^3}{\vartheta_f}}\frac{d^2}{d\eta^2}f(\eta)\right)\\ &= (a^2x)\left(\frac{d}{d\eta}f(\eta)\right)^2 + (-a^2x)f(\eta)\frac{d^2}{d\eta^2}f(\eta)\\ &= a^2x\left(\left(\frac{d}{d\eta}f(\eta)\right)^2 - f(\eta)\frac{d^2}{d\eta^2}f(\eta)\right) \qquad (3.3.14)\end{aligned}$$

Next is the right hand side of equation (3.1.2) and we have

$$\begin{aligned}RHS &= \frac{\mu_{hnf}}{\rho_{hnf}}\left(\frac{\partial^2 u}{\partial y^2}\right) + 2\vartheta_f\Lambda\left(\frac{\partial u}{\partial y}\right)\left(\frac{\partial^2 u}{\partial y^2}\right) + g\beta\big(T - T_{infty}\big) - \left(\frac{\sigma_{hnf}}{\rho_{hnf}}\right)B^2u\\ &= \frac{\mu_{hnf}}{\rho_{hnf}}\left(\frac{a^2x}{\vartheta_f}\frac{d^3f(\eta)}{d\eta^3}\right) + 2\vartheta_f\Lambda x\left(\sqrt{\frac{a^3}{\vartheta_f}}\right)\frac{d^2f(\eta)}{d\eta^2}\frac{a^2x}{\vartheta_f}\frac{d^3f(\eta)}{d\eta^3} + g\beta(T_w - T_\infty)\Theta(\eta)\\ &\quad -\frac{\sigma_{hnf}}{\rho_{hnf}}B^2\left(ax\frac{d}{d\eta}\ f(\eta)\right),\end{aligned}$$

$$= a^2 x\left(\frac{\mu_{hnf}}{\rho_{hnf}\vartheta_f}\frac{d^3 f(\eta)}{d\eta^3} + 2\Lambda a x\sqrt{\frac{a}{\vartheta_f}}\frac{d^2 f(\eta)}{d\eta^2}\frac{d^3 f(\eta)}{d\eta^3} + \frac{g\beta(T_w - T_\infty)}{a^2 x}\Theta(\eta)\right.$$
$$\left. - \frac{\sigma_{hnf}}{a\rho_{hnf}}B^2\frac{d}{d\eta}f(\eta)\right). \qquad (3.3.15)$$

Combining the left and right hand sides and equation (3.1.2) becomes

$$a^2 x\left(\left(\frac{d}{d\eta}f(\eta)\right)^2 - f(\eta)\frac{d^2}{d\eta^2}f(\eta)\right)$$
$$= a^2 x\left(\frac{\mu_{hnf}}{\rho_{hnf}\vartheta_f}\frac{d^3 f(\eta)}{d\eta^3} + 2\Lambda a x\sqrt{\frac{a}{\vartheta_f}}\frac{d^2 f(\eta)}{d\eta^2}\frac{d^3 f(\eta)}{d\eta^3} + \frac{g\beta(T_w - T_\infty)}{a^2 x}\Theta(\eta)\right.$$
$$\left. - \frac{\sigma_{hnf}}{a\rho_{hnf}}B^2\frac{d}{d\eta}f(\eta)\right) \qquad (3.3.16)$$

$$\left(\frac{d}{d\eta}f(\eta)\right)^2 - f(\eta)\frac{d^2}{d\eta^2}f(\eta)$$
$$= \frac{\mu_{hnf}}{\rho_{hnf}\vartheta_f}\frac{d^3 f(\eta)}{d\eta^3} + 2\Lambda a x\sqrt{\frac{a}{\vartheta_f}}\frac{d^2 f(\eta)}{d\eta^2}\frac{d^3 f(\eta)}{d\eta^3} + \frac{g\beta(T_w - T_\infty)}{a^2 x}\Theta(\eta)$$
$$- \frac{\sigma_{hnf}}{a\rho_{hnf}}B^2\frac{d}{d\eta}f(\eta) \qquad (3.3.17)$$

Now, by using equations (3.2.7) and (3.2.9), we have

$$\frac{\sigma_{hnf}}{a\rho_{hnf}} = \frac{A_2\sigma_f}{aA_4\rho_f}, \frac{\mu_{hnf}}{\rho_{hnf}\vartheta_f} = \frac{A_5\mu_f}{A_4\rho_f\vartheta_f} = \frac{A_5}{A_4} \qquad (3.3.18)$$

and the momentum equation becomes

$$\left(\frac{df}{d\eta}\right)^2 - f\frac{d^2 f}{d\eta^2} = \frac{A_5}{A_4}\frac{d^3 f}{d\eta^3} + 2\Lambda a x\sqrt{\frac{a}{\vartheta_f}}\frac{d^3 f}{d\eta^3}\frac{d^2 f}{d\eta^2} + \frac{g\beta(T_w - T_\infty)}{a^2 x}\Theta - \frac{A_2\sigma_f}{aA_4\rho_f}B^2\left(\frac{df}{d\eta}\right)$$

which is the same as

$$\frac{A_5}{A_4}\frac{d^3 f}{d\eta^3} + 2\Lambda a x\sqrt{\frac{a}{\vartheta_f}}\frac{d^3 f}{d\eta^3}\frac{d^2 f}{d\eta^2} - \left(\frac{df}{d\eta}\right)^2 + f\frac{d^2 f}{d\eta^2} + \frac{g\beta(T_w - T_\infty)}{a^2 x}\Theta - \frac{A_2\sigma_f}{aA_4\rho_f}B^2\left(\frac{df}{d\eta}\right) = 0$$
$$\left(\frac{A_5}{A_4} + 2\Lambda a x\sqrt{\frac{a}{\vartheta_f}}\frac{d^2 f}{d\eta^2}\right)\frac{d^3 f}{d\eta^3} - \left(\frac{df}{d\eta}\right)^2 + f\frac{d^2 f}{d\eta^2} + \frac{g\beta(T_w - T_\infty)}{a^2 x}\Theta - \frac{A_2\sigma_f}{aA_4\rho_f}B^2\left(\frac{df}{d\eta}\right) = 0$$

$$\left(\frac{A_5}{A_4}+2We\frac{d^2f}{d\eta^2}\right)\frac{d^3f}{d\eta^3}-\left(\frac{df}{d\eta}\right)^2+f\frac{d^2f}{d\eta^2}+Gr\Theta-\frac{A_2}{A_4}M\frac{df}{d\eta}=0 \qquad (3.3.19)$$

where

$$We=\Lambda ax\sqrt{\frac{a}{\vartheta_f}},\ \ Gr=\frac{g\beta(T_w-T_\infty)}{a^2x},\ \ M=\frac{\sigma_f B^2}{a\rho_f}.$$

Next stage is to consider the energy equation (3.1.3)

$$u\frac{\partial T}{\partial x}+v\frac{\partial T}{\partial y}-\frac{1}{(\rho c_p)_{hnf}}\left(\kappa_{hnf}\frac{\partial^2 T}{\partial y^2}+\frac{16\sigma^* T_\infty^3}{3k^*}\frac{\partial^2 T}{\partial y^2}-Q_0(T-T_w)\right)=0 \qquad (3.3.20)$$

and on substitutions, we have

$$0-\left(a^{\frac{1}{2}}\vartheta_f^{\frac{1}{2}}f(\eta)\right)\left(a^{\frac{1}{2}}\vartheta_f^{-\frac{1}{2}}(T_w-T_\infty)\frac{d}{d\eta}\Theta(\eta)\right)-\frac{1}{(\rho c_p)_{hnf}}\left(\kappa_{hnf}+\frac{16\sigma^* T_\infty^3}{3k^*}\right)\frac{a(T_w-T_\infty)}{\vartheta_f}\frac{d^2}{d\eta^2}\Theta(\eta)$$
$$+\frac{Q_0(T_w-T_\infty)}{(\rho c_p)_{hnf}}(\Theta-1)=0,$$
$$-\left(f(\eta)\frac{d}{d\eta}\Theta(\eta)\right)-\left(\frac{\kappa_{hnf}}{(\rho c_p)_{hnf}}+\frac{16\sigma^* T_\infty^3}{3k^*(\rho c_p)_{hnf}}\right)\frac{1}{\vartheta_f}\frac{d^2}{d\eta^2}\Theta(\eta)+\frac{Q_0(\Theta-1)}{a(\rho c_p)_{hnf}}=0.$$

Substituting equations (3.2.6) and (3.2.8)

$$-\left(f(\eta)\frac{d}{d\eta}\Theta(\eta)\right)-\left(\frac{A_1\kappa_f}{A_3(\rho c_p)_f\vartheta_f}+\frac{16\sigma^* T_\infty^3}{3k^*A_3(\rho c_p)_f\vartheta_f}\right)\frac{d^2}{d\eta^2}\Theta(\eta)+\frac{Q_0(\Theta-1)}{aA_3(\rho c_p)_f}=0. \quad (3.3.21)$$

Recall that the thermal diffusivity $\alpha_f$ of the base fluid is defined as $\alpha_f=\frac{\kappa_f}{(\rho c_p)_f}$ and so the equation becomes

$$-\left(f(\eta)\frac{d}{d\eta}\Theta(\eta)\right)-\left(\frac{A_1\alpha_f}{A_3\vartheta_f}+\frac{16\sigma^* T_\infty^3}{3k^*A_3(\rho c_p)_f\vartheta_f}\right)\frac{d^2}{d\eta^2}\Theta(\eta)+\frac{Q_0(\Theta-1)}{aA_3(\rho c_p)_f}=0. \qquad (3.3.22)$$

Also setting

$$\frac{1}{Pr}=\frac{\alpha_f}{\vartheta_f},\ \ R=\frac{4\sigma^* T_\infty^3}{k^*\vartheta_f(\rho c_p)_f} \quad \text{and} \quad Q=\frac{Q_0}{a(\rho c_p)_f}$$

we have

$$-\left(f(\eta)\frac{d}{d\eta}\Theta(\eta)\right)-\left(\frac{A_1}{A_3 Pr}+\frac{4}{3}R\right)\frac{d^2}{d\eta^2}\Theta(\eta)+\frac{Q}{A_3}(\Theta-1)=0,$$
$$\left(\frac{A_1}{A_3 Pr}+\frac{4}{3}R\right)\frac{d^2}{d\eta^2}\Theta(\eta)+\left(f(\eta)\frac{d}{d\eta}\Theta(\eta)\right)-\frac{Q}{A_3}(\Theta-1)=0 \qquad (3.3.23)$$

Finally, we consider the boundary conditions. Based on the choice of the similarity variables as $\eta=ya^{\frac{1}{2}}\vartheta_f^{-\frac{1}{2}}$, we

ISSN No. 2454-6194 | DOI: 10.51584/IJRIAS |Volume X Issue X October 2025

have

$$\text{at } y = 0, \ \ \eta = 0 \qquad \text{and as } y \to \infty, \eta \to \infty.$$

Starting at the wall where $y = 0$,

$$\begin{aligned} u(0,x) &= ax && \Rightarrow && \frac{df}{d\eta} = 1 \quad \text{at} \ \ \eta = 0 \\ v(0,x) &= 0 && \Rightarrow && f = 1 \quad \text{at} \ \ \eta = 0 \\ T(0,x) &= T_w && \Rightarrow && \Theta = 1 \quad \text{at} \ \ \eta = 0 \end{aligned}$$

At the free stream,

$$\begin{aligned} u(\infty,x) &\to 0 && \Rightarrow && f' \to 0 \quad \text{as} \quad \eta \to \infty \\ T(\infty,x) &\to T_\infty && \Rightarrow && \Theta \to 0 \quad \text{as} \quad \eta \to \infty \end{aligned}$$

The dimensionless equations are therefore

$$\left(\frac{A_5}{A_4} + 2We\frac{d^2f}{d\eta^2}\right)\frac{d^3f}{d\eta^3} - \left(\frac{df}{d\eta}\right)^2 + f\frac{d^2f}{d\eta^2} + Gr\Theta - \frac{A_2}{A_4}M\frac{df}{d\eta} = 0 \qquad (3.3.24)$$

$$\left(\frac{A_1}{A_3 Pr} + \frac{4}{3}R\right)\frac{d^2}{d\eta^2}\Theta(\eta) + f(\eta)\frac{d}{d\eta}\Theta(\eta) - \frac{Q}{A_3}(\Theta - 1) = 0 \qquad (3.3.25)$$

with the condition

$$f = 0, \ \ \frac{df}{d\eta} = 1, \ \ \Theta = 1 \quad \text{at} \ \ \eta = 0 \qquad (3.3.26)$$

$$f' \to 0, \qquad \Theta \to 0 \quad \text{as} \quad \eta \to \infty \qquad (3.3.27)$$

where

$$We = \Lambda ax\sqrt{\frac{a}{\vartheta_f}}, \ \ Gr = \frac{g\beta(T_w - T_\infty)}{a^2 x}, \ \ M = \frac{\sigma_f B^2}{a\rho_f} \qquad (3.3.28)$$

$$\alpha_f = \frac{\kappa_f}{(\rho c_p)_f}, \ \ \frac{1}{Pr} = \frac{\alpha_f}{\vartheta_f}, \ \ R = \frac{4\sigma^* T_\infty^3}{k^* \vartheta_f (\rho c_p)_f}, \ \ Q = \frac{Q_0}{a(\rho c_p)_f} \qquad (3.3.29)$$

**Thermophysical Properties**

The nanoparticles under study are that made from Molybdenum disulfide and silicon dioxide and the choice of base-fluid is molten polyethylene (a Maxwell fluid). The thermophysical properties of the base-fluid and that of the nanoparticles are obtained from literature and are recorded in table (3.1).

Table 3.1: Thermophysical properties

| | $\kappa$ | $\rho$ | $c_p$ | $\rho c_p$ | μ |
|---|---|---|---|---|---|
| $Al_2O_3$ | 40 | 3970 | 765 | 3037050 | - |
| $Cu$ | 400 | 8933 | 385 | 3439205 | - |
| molten polyethylene | 0.253 | 1115 | 2430 | 2709450 | 18.376 |

ISSN No. 2454-6194 | DOI: 10.51584/IJRIAS |Volume X Issue X October 2025

By substituting these values into equations (3.2.6 - 3.2.9), we have the following

$$A_1 = \frac{0.506(1-\phi)\phi + (1+2\phi)(34.5\phi_1 + 1.2\phi_2)}{0.253(2+\phi)\phi + (1-\phi)(34.5\phi_1 + 1.2\phi_2)},$$
$$A_2 = \frac{21.4(1-\phi)\phi \times 10^{-5} + (1+2\phi)(6.3\phi_1 + 4.25\phi_2) \times 10^7}{10.7(2+\phi)\phi \times 10^{-5} + (1-\phi)(6.3\phi_1 + 4.25\phi_2) \times 10^7},$$
$$A_3 = 1 - \phi + \frac{(2011147\phi_1 + 1546600\phi_2)}{2709450},$$
$$A_4 = 1 - \phi + \frac{(5060\phi_1 + 2200\phi_2)}{1115}.$$

**Numerical Procedure**

The coupled PDEs governing the MHD flow of hybrid nanofluid is reformulated as a coupled system of ODEs through the use of similarity transformation. The resulting the ODEs comes with some boundary conditions at the free stream and some initial conditions at the boundary layer. This kind of problem cannot be solved by simply adopting a numerical procedure due to the inclusion of boundary conditions. The problem concerning the boundary conditions is solved by bringing in the method of Shooting Technique; which seeks the initial condition that best satisfies the boundary condition. The Runge Kutta method is used to solve the coupled ODEs with the initial conditions. The numerical results are graphed and the results are discussed herewith.

**Analysis of Results**

**Introduction**

The parameters that emerged from the nondimensionalisation process are varied to simulate the flow. By varying a parameter while fixing other parameters, the profiles for velocity and temperature of the flow are plotted against the dimensionless distance $\eta$. In any case a parameter is fixed, the following values are chosen as the default for the parameters;

$$We = 0.1,\ \ Gr = 1,\ \ M = 2,\ \ Pr = 7,\ \ Q = 0.21,\ \ R = 0.1,\ \ \phi_1 = \phi_2 = 0.1.$$

Recall that the flow velocity is similar to $f'$ and temperature is similar to $\Theta$, hence, in the following discussion, the same notations shall be retained for these flow properties.

## RESULTS AND DISCUSSION

The parameters that emerged from the nondimensionalisation process are varied to simulate the flow. By varying a parameter while fixing other parameters, the profiles for velocity and temperature of the flow are plotted against the dimensionless distance $\eta$. In any case a parameter is fixed, the following values are chosen as the default for the parameters;

$$We = 0.1,\ \ Gr = 1,\ \ M = 2,\ \ Pr = 7,\ \ Q = 0.21,\ \ R = 0.1,\ \ \phi_1 = \phi_2 = 0.1.$$

Recall that the flow velocity is similar to $f'$ and temperature is similar to $\Theta$, hence, in the following discussion, the same notations shall be retained for these flow properties.

**Effect of Grashof Number**

The Grashof number $Gr$ measures the ratio of buoyancy to viscous forces, often arising in natural convection and defined in this study as

$$Gr = \frac{g\beta(T_w - T_\infty)}{a^2 x}.$$

The behaviour of temperature with increasing Grashof number is shown in figure (4.1) while the behaviour of velocity is illustrated in figure (4.2). The figures illustrated a decrease in temperature and an increase in velocity with Grashof number. A rise in Grashof number is a consequence of increasing buoyancy force which enhances flow velocity but reduces thermal boundary layer. Hence, as Grashof number rises, temperature goes down and velocity goes up.

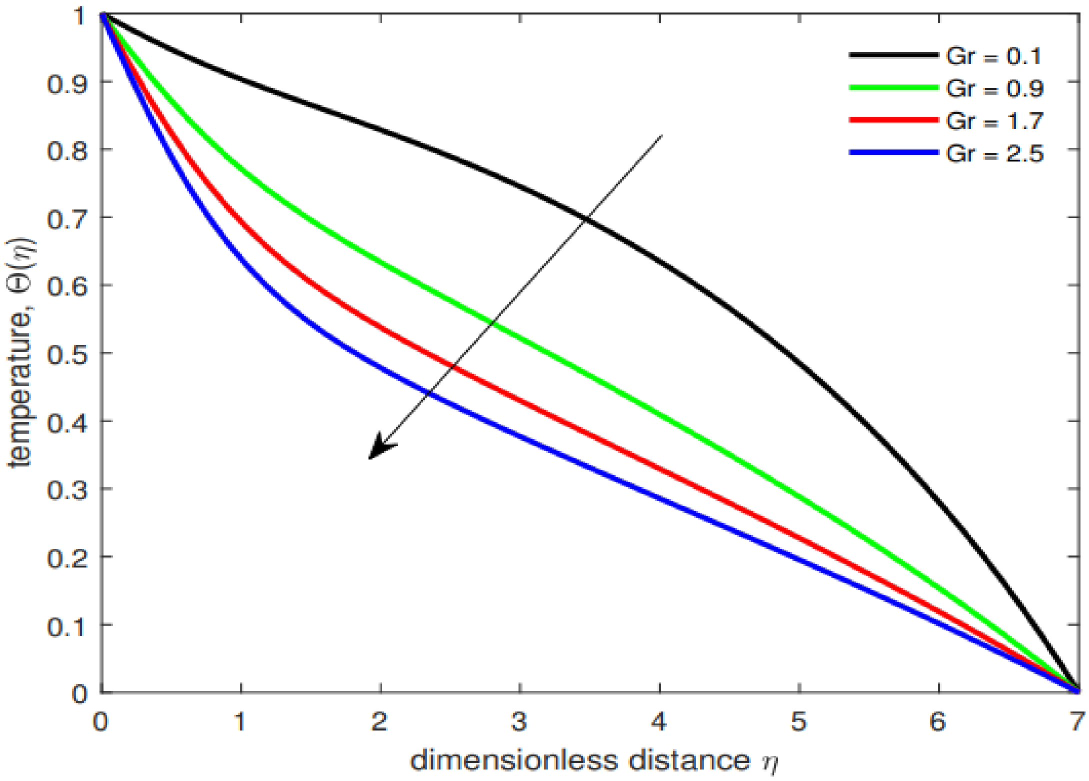


Figure 4.1: Effects of temperature to Grashof number

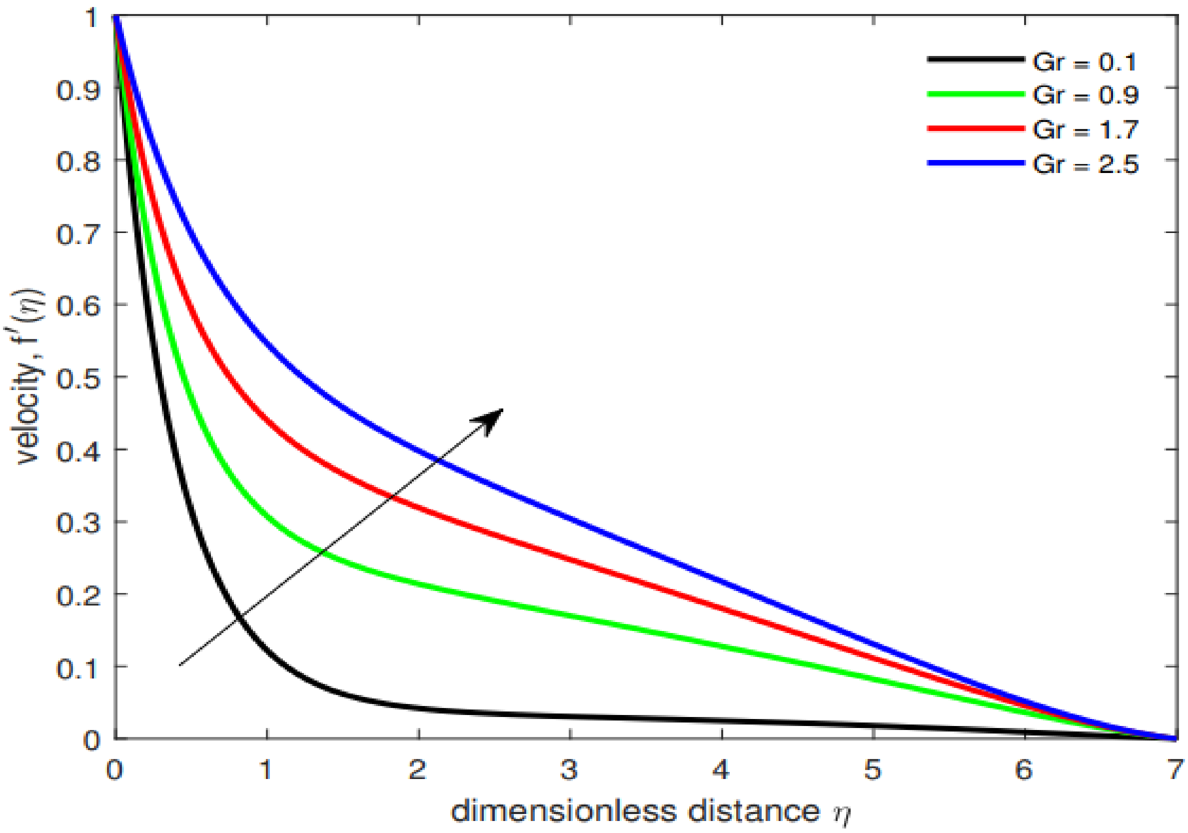


Figure 4.2: Effects of Velocity to Grashof number

**Effect of Magnetic field**

A magnetised hybrid nanofluid flow experiences an opposing force called Lorenz force. This implies that Lorenz force becomes stronger as magnetism increases and therefore, the flow experiences more opposition. In this study, the magnitude of magnetism is obtained as

$$M = \frac{\sigma_f B^2}{a\rho_f}.$$

We increase *M*, consequently increasing Lorenz force, and study the response of temperature and velocity to increasing magnetism. Figures (4.3) and (4.4) display the behaviours. The stronger the magnetism, the higher the temperature becomes but the lower the velocity. Fluid motion get impeded by the Lorenz force and thereby slow down the fluid particles, causing a reduction in velocity. The drag in the flow produce thermal energy which increases the temperature if the flow, hence an increase in flow temperature.

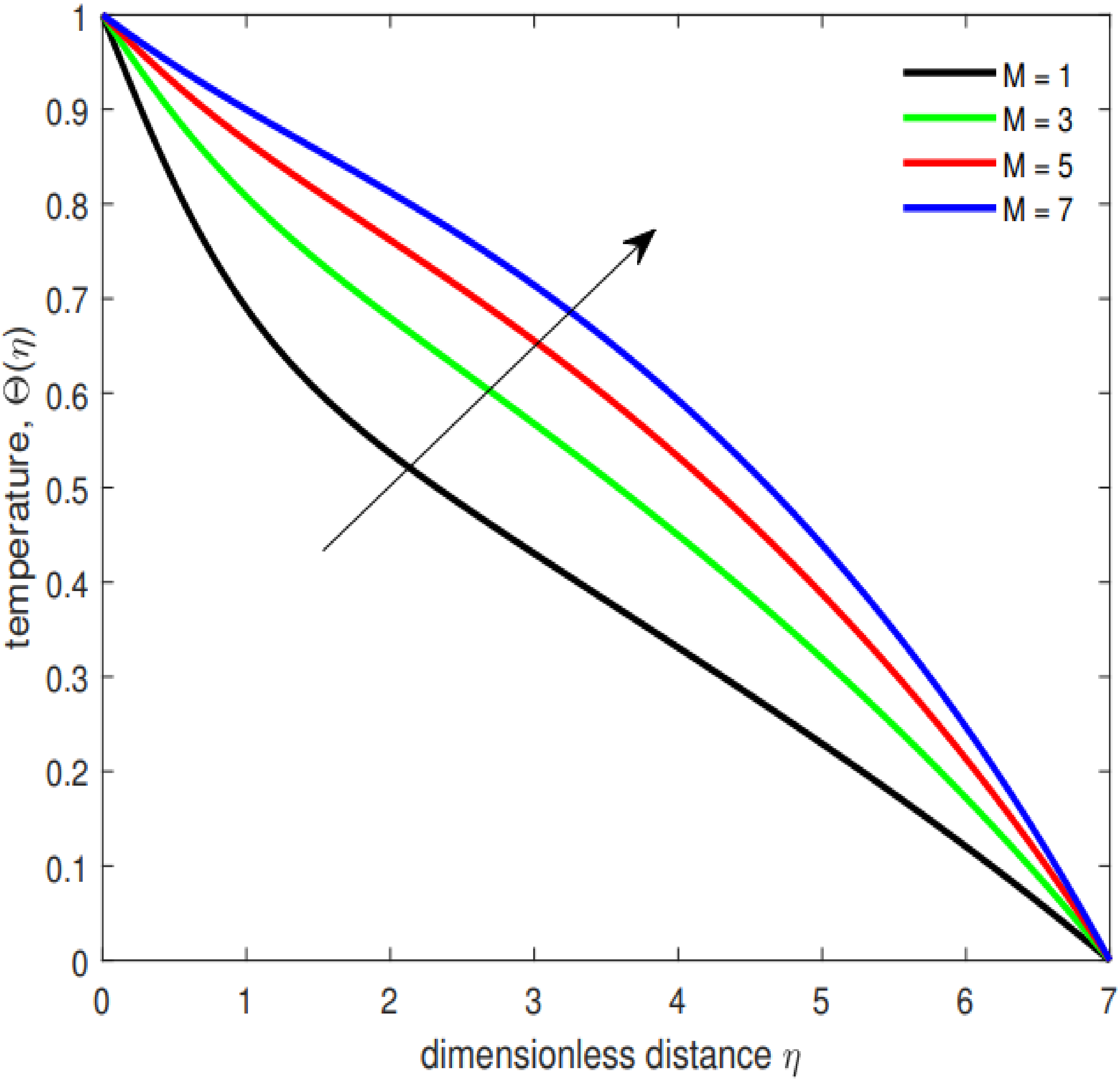


Figure 4.3: Effects of Temperature to Magnetism

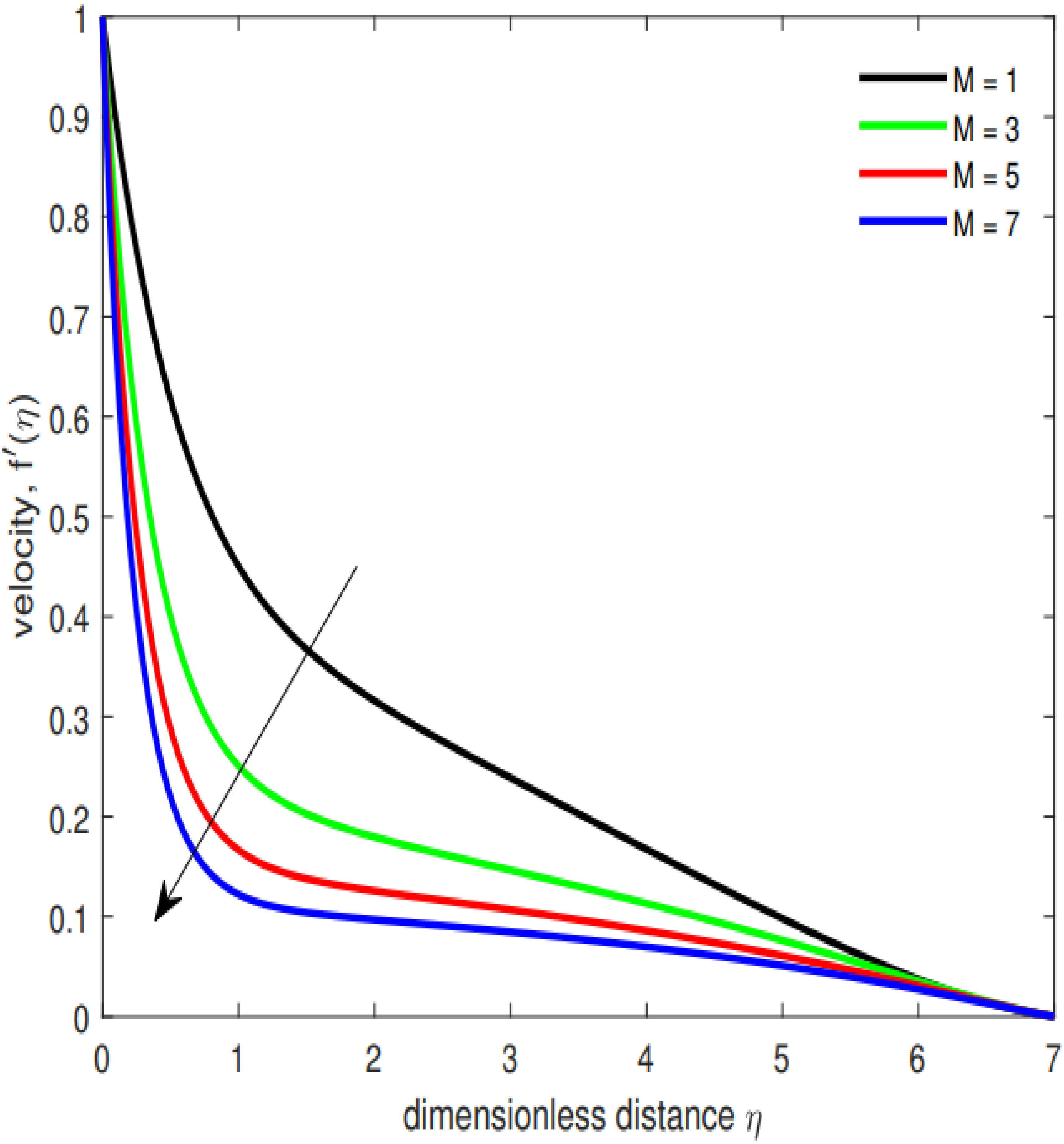


Figure 4.4: Effects of Temperature to Magnetism

**Effect of Volume Fraction**

The volume fractions for the nanoparticles are $\phi_1$ and $\phi_2$, where 1 represents $MoS_2$ nanoparticles and 2 represents silicon dioxide. In this study, we have considered only the case where the two volume fractions are equal $\phi_1 = \phi_2$. Figure (4.5) shows the behaviour of the temperature of flow as $\phi_1$ and $\phi_2$ increase. The temperature increases as $\phi_1$ and $\phi_2$ get bigger. Increasing $\phi_1$ and $\phi_2$ increases the surface area of the solid particles and thereby allowing quick exchange of heat energy. This is responsible for the rise in temperature as $\phi_1$ and $\phi_2$ increase. However, figure (4.6) shows that velocity decreases with increasing $\phi_1$ and $\phi_2$. Due to the increase in $\phi_1$ and $\phi_2$, nanoparticles agglomeration tends to cause a retardation in the flow and thereby reducing velocity as $\phi_1$ and $\phi_2$ gets larger.

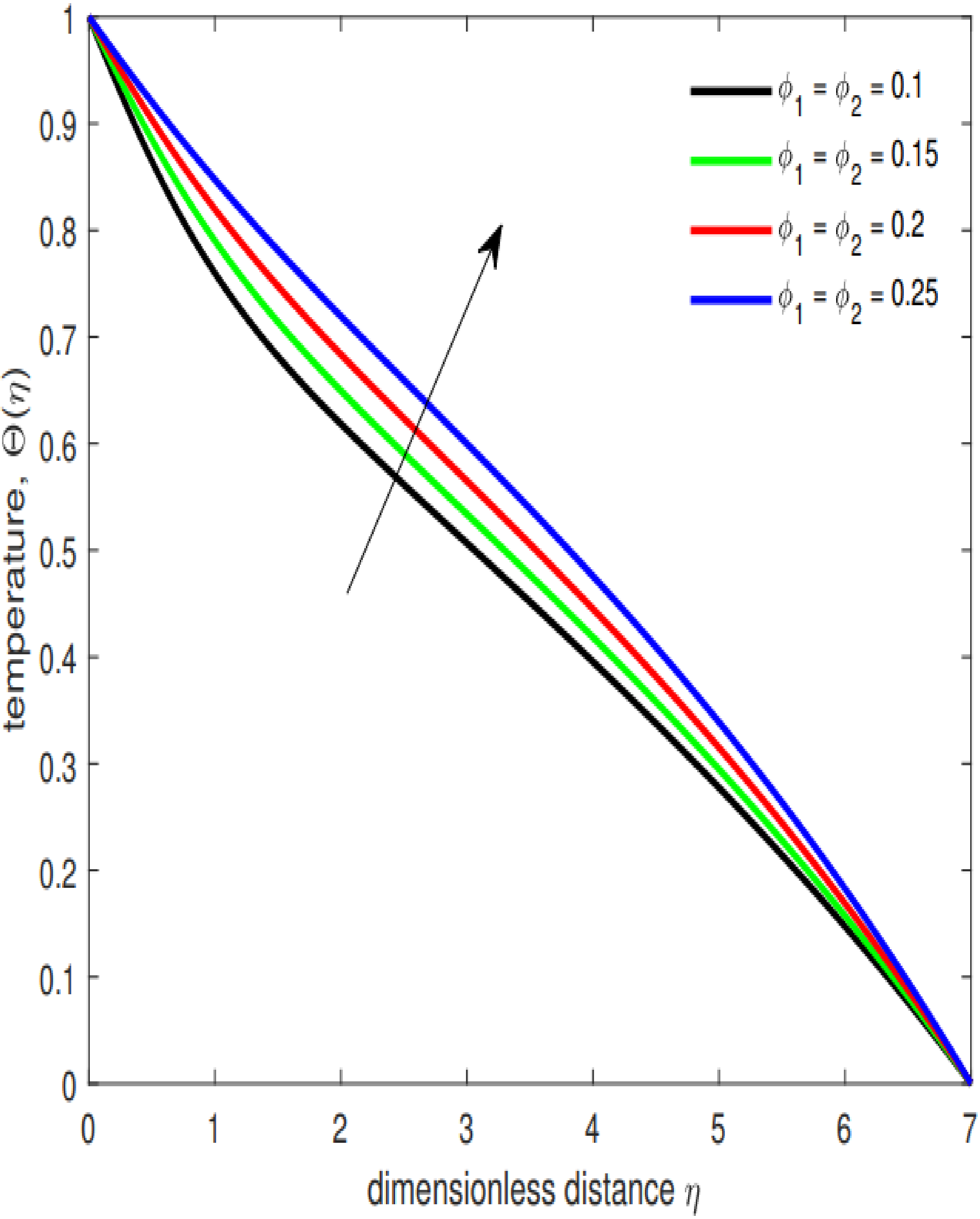


Figure 4.5: Effects of Temperature to Volume fractions

ISSN No. 2454-6194 | DOI: 10.51584/IJRIAS |Volume X Issue X October 2025

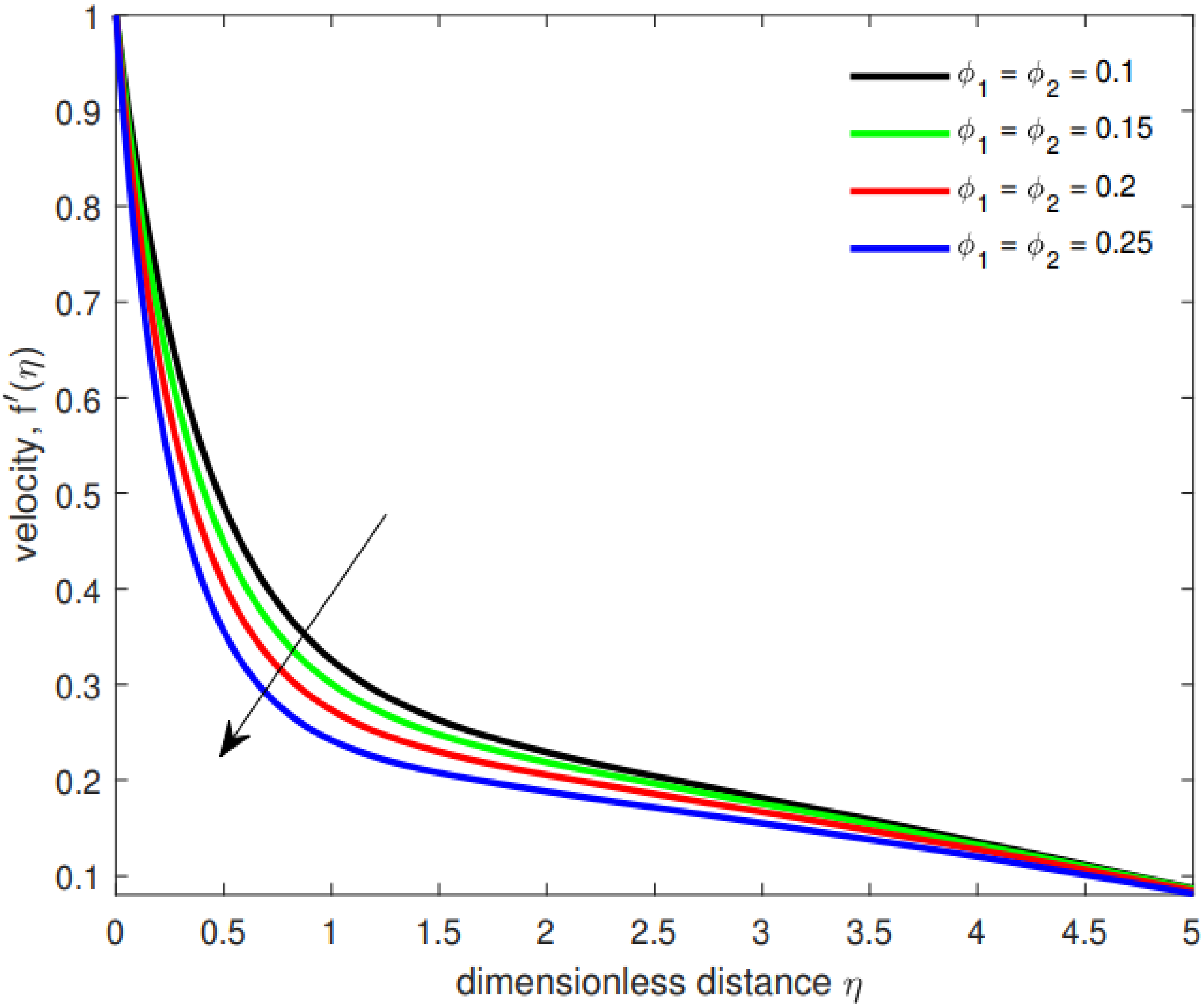


Figure 4.6: Effects of Velocity  to Volume fractions

## CONCLUSION AND RECOMMENDATION

### Conclusion

This study considers the flow of fluid obtained by releasing two nanoparticles of different solid materials in the molten polyethylene. The flow is represented in mathematical form as a coupled PDE with some initial-boundary condition, which is reformulated as a coupled ODEs by the use of similarity transformation. We employed the shooting technique to find an analogous the initial value problem to the initial-boundary condition problem. By varying a parameter while keeping other parameter fixed, the flow is simulated and the following results were obtained;

- Decrease in temperature and increase in velocity with Grashof number: As the Grashof number increases, indicating stronger buoyancy forces relative to viscous forces, the temperature decreases. This is because the fluid experiences less resistance from buoyancy, allowing it to flow more freely and increase in velocity.
- Magnetism raises temperature but lowers velocity: The introduction of magnetism increases the fluid temperature due to heat generation from magnetic nanoparticles. However, it also decreases fluid velocity, possibly due to altered flow patterns or increased frictional forces.
- Temperature increases but velocity decreases as volume fraction increases: Higher nanoparticle concentration leads to increased fluid temperature due to enhanced thermal conductivity or heat generation. However, the fluid velocity decreases as nanoparticles impede flow, causing greater resistance.

# RECOMMENDATION

**Based on the findings of this study, the following are recommended:**

1. There is a crucial need for experimental validation of the simulation results. Conducting rigorous experiments would not only validate the accuracy of the model but also provide a real-world context for understanding the observed phenomena. By comparing simulation results with experimental data, researchers can gain confidence in the predictive capabilities of the model and refine it further.
2. Exploring the effects of varying nanoparticle properties, such as size, shape, and surface characteristics, could yield valuable insights. Understanding how these factors influence fluid behaviour and thermal dynamics could lead to the development of optimized nanoparticle designs for specific applications. This avenue of research has the potential to unlock new possibilities in areas such as heat transfer enhancement and nanofluid-based technologies.
3. In addition to nanoparticle properties, investigating the impact of external factors on the system is essential. Factors such as pressure variations, different fluid compositions, or external fields could significantly influence fluid flow and temperature distribution. Exploring these factors could not only expand the scope of potential applications but also enhance our understanding of the system's robustness and adaptability.

# REFERENCES

1. Alfvén, H. (1942). Existence of Electromagnetic-Hydrodynamic Waves. Nature, 150(3805):405–406.
2. Ali, A., Kanwal, T., Awais, M., Shah, Z., Kumam, P., and Thounthong, P. (2021). Impact of thermal radiation and non-uniform heat flux on MHD hybrid nanofluid along a stretching cylinder. Scientific Reports, 11(1).
3. Ali, B., Ahammad, N. A., Awan, A. U., Oke, A. S., Tag-ElDin, E. M., Shah, F. A., & Majeed, S. (2022). The dynamics of water-based nanofluid subject to the nanoparticle's radius with a significant magnetic field: The case of rotating micropolar fluid. Sustainability, 14(17), 10474.
4. Allehiany, F. M., Bilal, M., Alfwzan, W. F., Ali, A., and Eldin, S. M. (2023). Numerical solution for the electrically conducting hybrid nanofluid flow between two parallel rotating surfaces subject to thermal radiation. AIP Advances, 13(7).
5. Asghar, A., Lund, L. A., Shah, Z., Vrinceanu, N., Deebani, W., and Shutaywi, M. (2022). Effect of thermal radiation on three-dimensional magnetized rotating flow of a hybrid nanofluid. Nanomaterials, 12(9):1566.
6. Choi, U. S. and Eastman, J. (1995). Enhancing Thermal Conductivity of Fluids with Nanoparticles. ASME International Mechanical Congress and Exposition, San Francisco, (12–17).
7. Farooq, U., Lu, D., Munir, S., Ramzan, M., Suleman, M., and Hussain, S. (2019). MHD flow of maxwell fluid with nanomaterials due to an exponentially stretching surface. Scientific Reports, 9(1).
8. Fatunmbi, E. O., Badru, J. O., & Oke, A. S. (2020). Magneto-Reactive Jeffrey Nanofluid Flow over a Stretching Sheet with Activation Energy, Nonlinear Thermal Radiation and Entropy Analysis.
9. Hady, F. M., Ibrahim, F. S., Abdel-Gaied, S. M., and Eid, M. R. (2012). Radiation effect on viscous flow of a nanofluid and heat transfer over a nonlinearly stretching sheet. Nanoscale Research Letters, 7(1).
10. Jaafar, A., Waini, I., Jamaludin, A., Nazaar, R., and Pop, I. (2022). Mhd flow and heat transfer of a hybrid nanofluid past a nonlinear surface stretching/shrinking with effects of thermal radiation and suction. Chinese Journal of Physics, 79:13–27.
11. Khan, N., Ali, F., Ahmad, Z., Murtaza, S., Ganie, A. H., Khan, I., & Eldin, S. M. (2023). A time fractional model of a Maxwell nanofluid through a channel flow with applications in grease. Scientific Reports, 13(1), 4428.
12. Kigio, J. K., Mutuku, W. N., & Oke, A. S. Analysis of volume fraction and convective heat transfer on MHD Casson nanofluid over a vertical plate, Fluid Mechanics, 7 (2021), 1–8.
13. Maxwell, J. C. (1873). A Treatise on Electricity and Magnetism. Nature, 7:478–480.
14. Rajesh, V., Srilatha, M., and Chamkha, A. J. (2020). Hydromagnetic effects on hybrid nanofluid (cu–aluminium-water) flow with convective heat transfer due to a stretching sheet. Journal of Nanofluids, 9(4):293–301.

ISSN No. 2454-6194 | DOI: 10.51584/IJRIAS |Volume X Issue X October 2025


15. Sakiadis, B. C. (1961). Boundary-layer behavior on continuous solid surfaces: I. boundary-layer equations for two-dimensional and axisymmetric flow. AIChE Journal, 7(1):26–28.
16. SAMUEL, O. A. (2022). Coriolis Effects on Air, Nanofluid and Casson Fluid Flow Over a Surface with Nonuniform Thickness. PhD diss., KENYATTA UNIVERSITY
17. Suresh, S., Venkitaraj, K., Selvakumar, P., and Chandrasekar, M. (2011). Synthesis of al2o3–cu/water hybrid nanofluids using two step method and its thermo physical properties. Multidisciplinary Digital, 388(1-3):41–48.
18. Vijay, N., & Sharma, K. (2023). Dynamics of stagnation point flow of Maxwell nanofluid with combined heat and mass transfer effects: A numerical investigation. International Communications in Heat and Mass Transfer, 141, 106545.
19. Wang, F., Jamshed, W., Ibrahim, R. W., Abdalla, N. S. E., Abd-Elmonem, A., & Hussain, S. M. (2023). Solar radiative and chemical reactive influences on electromagnetic Maxwell nanofluid flow in Buongiorno model. Journal of Magnetism and Magnetic Materials, 576, 170748.
20. Zainal, N. A., Nazar, R., Naganthran, K., and Pop, I. (2022). The impact of thermal radiation on maxwell hybrid nanofluids in the stagnation region. Multidisciplinary Digital Publishing Institute.

ISSN No. 2454-6194 | DOI: 10.51584/IJRIAS |Volume X Issue X October 2025

# APPENDIX

## Declaration

### Declaration by the Candidate

This proposal is my original work and has not been submitted for any award of a degree in any University.

**Name:** Francis Kirwa Korir

**Signature:** ........................................ **Date:** ..................................................

### Declaration by the Supervisor

This proposal has been submitted for examination with my approval as the University

**Name:** Prof W. N. Mutuku

**Signature:** ........................................ **Date:** ..................................................

Department of Mathematics and Actuarial Science Kenyatta University.

## Nomenclature

| | | | |
|---|---|---|---|
| $u, v$ | velocities in the $x, y$-directions | $\rho$ | Density |
| $v$ | kinematic viscosity | $\sigma^*$ | Boltzmann constant |
| $\Lambda$ | Maxwell parameter | $k^*$ | mean absorption coefficient |
| $q$ | radiative heat flux | $\alpha$ | thermal diffusivity |
| $g$ | gravitational acceleration | $T$ | temperature |
| $\beta$ | thermal expansivity | $c_p$ | Specific heat capacity |
| $\sigma$ | electric conductivity | $B$ | magnetic field strength |
| $T_\infty$ | Free stream temperature | $\mu$ | viscosity coefficient |
| $We$ | Weber | $\phi$ | volume fraction |
| $R$ | Radiation parameter | $Gr$ | Grashof number |

**The MATLAB Code**

```
clc; clear all; format compact

global We Gr M Pr R Q phi mu_f phi kappa sigma rho cp

mu_f = 18.376; We = 0.1; Gr = 1; M = 2; Pr = 7; Q = 0.21; R = 0.1;

phi = [0.1, 0.1]; tspan=linspace(0,7,500); x_initial = zeros(1,5); i=1;

%nanoparticles are Al2O3 and Cu

%base fluid is molten polyethylene

kappa = [40, 400, 0.253]; sigma = [6.3e7,4.25e7,10.7e-5];

rho = [3970, 8933, 1115]; cp = [765, 385, 2430];

Legend_Entries = []; txt_var = "phi"; Line_Style = ["k-", "g-", "r-", "b-"];

for Val = [0.1, 0.15, 0.2, 0.25]

   phi = [Val, Val];

   solinit=bvpinit(tspan,x_initial);

   sol = bvp4c(@Fluid,@Bc,solinit);

   t = sol.x; s = sol.y;

   %Legend_Entries = [Legend_Entries,strcat(txt_var," = ", num2str(Val))];

   Legend_Entries = [Legend_Entries,strcat("\phi_1 = \phi_2 = ", num2str(Val))];

   txt = Line_Style(i);

      if i ~= 4

      figure(2), plot(t,s(2,:),txt,'LineWidth',2)

      hold on

      figure(4), plot(t,s(4,:),txt,'LineWidth',2)

      hold on

   elseif i == 4
```

ISSN No. 2454-6194 | DOI: 10.51584/IJRIAS |Volume X Issue X October 2025

```
        figure(2), plot(t,s(2,:),txt,'LineWidth',2)

        xlabel(" dimensionless distance \eta")

        ylabel("velocity, f^\prime(\eta)")

        legend(Legend_Entries); legend('boxoff')

        txt_vel = strcat(txt_var,"_velocity");

        saveas(gcf,txt_vel,'fig')

        figure(4), plot(t,s(4,:),txt,'LineWidth',2)

        xlabel(" dimensionless distance \eta")

        ylabel("temperature, \Theta(\eta)")

        legend(Legend_Entries); legend('boxoff')

        txt_temp = strcat(txt_var,"_temperature");

        saveas(gcf,txt_temp,'fig')

    end

    i=i+1;

end

function res = Fluid(eta,x)

global We Gr M Pr R Q phi mu_f phi kappa sigma rho cp

    f = x(1); f_p = x(2); f_pp = x(3); theta = x(4); theta_p = x(5);

    PHI = sum(phi);

    A1_num = 2*(1-PHI)*PHI*kappa(3) + (1 + 2*PHI)*sum(phi.*kappa(1:2));

    A1_den = (2+PHI)*PHI*kappa(3) + (1 - PHI)*sum(phi.*kappa(1:2));

    A1 = A1_num/A1_den;

    A2_num = 2*(1-PHI)*PHI*sigma(3) + (1 + 2*PHI)*sum(phi.*sigma(1:2));

    A2_den = ((2+PHI)*PHI*sigma(3) + (1 - PHI)*sum(phi.*sigma(1:2)));
```

```
    A2 = A1_num/A1_den;

%    A2 = (1-PHI + sum(phi.*sigma(1:2))/sigma(3));

    A3 = 1 - PHI + sum(phi.*rho(1:2).*cp(1:2))/(rho(3)*cp(3));

    A4 = 1 - PHI + sum(phi.*rho(1:2))/rho(3);

    A5 = 0.904*exp(0.148*PHI);

    dx1 = x(2); dx2 = x(3);

    dx3 = (f_p^2 - f*f_pp - Gr*theta + (A2/A4)*M*f_p)/((A5/A4) + We*f_pp);

    dx4 = x(5);

    dx5 = (-f*theta_p + Q*(theta - 1)/A3)/(A1/(A3*Pr) + (4*R/3));

    res = [dx1, dx2, dx3, dx4, dx5];

end

function res = Bc(y0,yinf)

global We Gr M Pr R Q phi mu_f phi kappa sigma rho cp

    res = [y0(1)

        y0(2)-1

        y0(4)-1

        yinf(2)

        yinf(4)];

end
```